The Journal of Experimental Biology 208, 4363-4376
Published by The Company of Biologists 2005
doi:10.1242/jeb.01911

Transepithelial transport of fluorescent p-glycoprotein and MRP2 substrates by insect Malpighian tubules: confocal microscopic analysis of secreted fluid droplets

J. P. Leader and M. J. O'Donnell*

Department of Physiology, University of Otago, New Zealand

*Author for correspondence at present address: Department of Biology, McMaster University, 1280 Main Street West, Hamilton, ON, Canada L8S 4K1 (e-mail: odonnell@mcmaster.ca)

Accepted 3 October 2005

Summary

Transport of fluorescent substrates of p-glycoprotein (P-gp) and multidrug resistance-associated protein 2 (MRP2) by insect Malpighian tubules was examined using confocal laser scanning microscopy (CLSM). Isolated tubules of the cricket *Teleogryllus commodus* accumulated the MRP2 substrate Texas Red in the cells and lumen at concentrations up to 20 and 40 times, respectively, those in the bathing medium. Quantitative CLSM analysis of fluorochrome transport in some cricket tubules and all *Drosophila* tubules was not practical because of interfering effects of concretions in the cells and lumen. Samples of fluid secreted by tubules set up in Ramsay assays were therefore collected in hollow rectangle glass capillaries. Transepithelial dye flux was calculated as the product of fluid secretion rate (measured in the Ramsay assay) and dye concentration (measured by CLSM of the fluid samples). Dose–response curves for transport and the ratio of dye concentration in the secreted fluid to that in the bathing medium (S/M) were determined for Texas Red as well as for P-gp substrates (rhodamine 123, daunorubicin), the organic anion fluorescein and the organic cation quinacrine. Transepithelial transport of Texas Red was reduced by the MRP2 inhibitors MK571 and probenecid. Transport of daunorubicin was reduced by the P-gp inhibitors verapamil and quinacrine and also by the organic cation tetraethylammonium. The results indicate the presence of P-gp-like and MRP2-like transporters in the Malpighian tubules of both species.

Key words: p-glycoprotein, multidrug resistance associated protein, Malpighian tubule, confocal microscopy.

Introduction

P-glycoprotein (P-gp) and multidrug resistance-associated proteins (MRPs) are integral membrane proteins that act as ATP-dependent efflux pumps in tissues such as the gut, kidney, liver and blood–brain barrier. They have been implicated in resistance of many organisms to a vast and chemically diverse range of toxic molecules. P-gps are the products of multidrug resistance (*MDR*) genes and they transport neutral or cationic amphiphilic compounds. MRPs transport neutral, cationic or anionic compounds and are also important in the transport of anionic conjugates of amphiphilic compounds with glutathione, glucuronide or sulphate (Bard, 2000).

P-glycoproteins in insects merit study because such transporters may contribute to insecticide resistance. Organochlorine and organophosphorous pesticides such as chlorpyrifos bind to P-gp, and exposure to such compounds increases *MDR* gene expression (Bain and LeBlanc, 1996; Lanning et al., 1996). Exposure to the P-gp inhibitor verapamil increases the toxicity of ivermectin in chironomids (Podsiadlowski et al., 1998) and the toxicity of three insecticide classes (cypermethrin, ivermectin and endosulphan) in mosquitoes (Buss et al., 2002).

A few studies have examined the possible role of P-gps and MRPs in the Malpighian tubules (MTs) of insects. Although there are, to date, no functional studies of P-gps in the MTs of the fruit fly *Drosophila melanogaster*, three *MDR* genes have been identified (Wu et al., 1991; Gerrard et al., 1993), and deduced amino acid sequences are ~40% identical to those of mammalian homologs. P-glycoprotein-like transporters in the MTs of the tobacco hornworm, *Manduca sexta*, transport P-gp substrates such as nicotine and vinblastine into the lumen, and transport is reduced by the P-gp inhibitor verapamil (Gaertner et al., 1998). Immunofluorescence studies have also indicated the presence of P-gp-like proteins in the MTs (Murray et al., 1994). However, although fluorescent P-gp substrates such as daunorubicin (daunomycin) and rhodamine 123 are taken up into the tubule cells of *Manduca*, these fluorochromes do not appear in the lumen of isolated tubules examined using confocal laser scanning microscopy (CLSM; Gaertner and Morris, 1999). These authors suggested that reflection, refraction or absorption of exciting or emitted wavelengths by structures such as uric acid crystals in the lumen may have prevented detection of the fluorescent compounds in the lumen.

MRPs have been identified in the MTs of the cockroach *Periplaneta americana* and the cricket *Acheta domesticus* (Karnaky et al., 2000, 2001, 2003). MTs of both species transport the fluorescent MRP2 substrate Texas Red (sulphorhodamine 101) through the cells and into the lumen. Confocal microscopic studies of isolated MTs indicate that the concentration of the fluorochrome in the lumen is dependent upon metabolism and is inhibited by the non-fluorescent MRP2 substrate chlorodinitrobenzene. An ortholog of human *MRP* genes has been identified in *Drosophila*, although transport of MRP substrates by the MTs has not been tested. The *Drosophila* MRP (*dMRP*) gene contains 19 exons that are alternatively spliced, resulting in multiple isoforms (Tarnay et al., 2004).

The present study describes secretion of fluorescent P-gp and MRP substrates by the MTs of two insect species. Isolated tubules were set up in Ramsay secretion assays and nanolitre samples of secreted fluid were collected in optically flat glass capillaries. The concentration of fluorescent P-gp and MRP substrates was determined using CLSM. The analysis of secreted droplets circumvents many of the problems associated with analysis of isolated tubules, in which the presence of opaque concretions in the cells and/or lumen interferes with CLSM. In addition, measurements of fluid secretion rate during flux measurements permit non-specific toxicity of inhibitors of P-gps and MRPs, or of high concentrations of the fluorescent compounds themselves, to be distinguished from specific inhibition of multidrug-resistant transporters. We report here the first measurements of the transepithelial flux for P-gp and MRP2 substrates across isolated MTs. Flux is calculated as the product of fluid secretion rate, determined in the Ramsay assay, and the concentration of the compound of interest in the secreted fluid. We have determined kinetic parameters (J_{max} and K_t) for transport of P-gp and MRP2 substrates. We also show that the method is suitable for fluorescent substrates of other transporters, such as those involved in transepithelial secretion of organic anions such as fluorescein and organic cations such as quinacrine.

Materials and methods

Insect cultures and physiological salines

Drosophila melanogaster (Meigen) were raised on standard yeast medium using protocols described by Ashburner (1989). Malpighian tubules were dissected under saline from adult females aged 3–14 days, as described by Dow et al. (1994). Experiments were performed at room temperature (17–23°C). The control saline contained (in mmol l^{-1}); NaCl (117.5), KCl (20), $CaCl_2$ (2), $MgCl_2$ (8.5), $NaHCO_3$ (10.2), NaH_2PO_4 (4.3), Hepes (8.6), L-glutamine (10) and glucose (20). Saline was titrated to pH 7 with NaOH. A sodium-free saline contained *N*-methyl D-glucamine chloride (117.5), KCl (5), $KHCO_3$ (10.2), KH_2PO_4 (4.3) and the same concentrations of $CaCl_2$, $MgCl_2$, Hepes, L-glutamine and glucose as control saline. Na-free saline was titrated to pH 7 with HCl.

Crickets (*Teleogryllus commodus* Walker) were obtained from Biosuppliers (Auckland, New Zealand) and were maintained on ground Purina rat chow and water *ad libitum*, supplemented with lettuce leaves. Tubules were dissected from last instar larvae and adult males under saline containing (in mmol l^{-1}) NaCl (100), KCl (8.6), $CaCl_2$ (1.5), $MgCl_2$ (8.5), $NaHCO_3$ (4), NaH_2PO_4 (4.0), Hepes (25), L-glutamate (10), sucrose (56) and glucose (24). Saline was titrated to pH 7 with NaOH.

Ramsay assays and collection of fluid secreted by isolated Malpighian tubules

Isolated tubules of each species were transferred to 20 μl droplets of saline under paraffin oil for Ramsay assays. One tubule of each pair of isolated *Drosophila* tubules was pulled out of the bathing droplet and wrapped around a steel minuten pin (0.15 mm diameter) stuck into the Sylgard™ bottom of the assay dish. The lower tubule and ureter were positioned outside of the bathing saline, so that the composition of the secreted fluid was determined by transport activity of the main segment only. The lower tubule was readily identified by the absence of stellate cells. Secreted droplets formed at the end of the ureter and were collected after 45–60 min with a fine glass probe. Droplet diameters (*d*) were measured using an ocular micrometer, and droplet volume (nl) was calculated as $\pi d^3/6$. Secretion rate (nl min^{-1}) was calculated by dividing the droplet volume by the time (min) over which the droplet formed.

The blind end of each cricket tubule was placed in the saline droplet and the open end, formed where the tubule was broken from its junction with the ampulla, was wrapped around a steel pin. The tubule was then squeezed between forceps at a point halfway between the pin and the droplet, thereby rupturing the tubule wall and permitting the escape of secreted fluid.

For analysis by CLSM, secreted droplets were collected in optically flat hollow rectangle glass capillaries (VitroTubes; VitroCom, Mountain Lakes, NJ, USA). Most of the experiments described below used borosilicate capillaries with a path length of 50 μm, a wall thickness of 50 μm and a width of 500 μm. Capillaries were supplied in 50 mm lengths and were scored with the edge of a carborundum stone and broken into lengths of 8–10 mm. Some experiments used capillaries with a path length of 20 μm, wall thickness of 20 μm and width of 200 μm. Capillaries were held with forceps and inserted through the paraffin oil of the Ramsay assay dish and into a droplet of secreted fluid or calibration solution. The aqueous sample was taken up by capillarity and was thus enclosed by glass on four sides and by paraffin oil on two sides. Luminal concretions were sometimes expelled into the droplets secreted during the Ramsay assay. The concretions settled to the bottom of the droplet and were not collected when the fluid was taken up into the hollow rectangle glass capillary.

For *Drosophila*, transepithelial dye flux (fmol min^{-1} $tubule^{-1}$) was calculated by multiplying fluid secretion rate (nl min^{-1} $tubule^{-1}$) by the dye concentration (μmol l^{-1}) measured by CLSM. Cricket tubules varied in length by >25% within an individual and in different insects. Moreover, vigorous contractions of the muscles in each cricket

tubule prevented precise measurement of tubule length, so we could not normalize fluid secretion rates per unit length. We therefore report only secreted fluid dye concentrations rather than dye flux for individual cricket tubules. However, approximate values for transepithelial dye flux across cricket tubules could be estimated from secreted fluid dye concentration and a mean secretion rate based on measurements of >50 tubules from several insects.

Confocal laser scanning microscopy

A chamber made from a 6-well tissue culture dish was used for CLSM of MTs or optically flat glass capillaries. A 15 mm hole was drilled in the centre of each well and a 22 mm square glass cover slip was secured across the opening with melted dental wax. The cover slips were pre-coated with 100 μl droplets of 125 μg ml^{-1} poly-L-lysine (70 kDa) to facilitate adherence of isolated MTs. Tubules were transferred into 2 ml saline in the bottom of each well and Texas Red was added from stock solutions to achieve concentrations of 0.5 μmol l^{-1} to 50 μmol l^{-1}. Glass capillaries containing secreted fluid or calibration solutions were placed in empty wells on uncoated glass cover slips.

Confocal fluorescent images were obtained with a Zeiss LSM 510 confocal microscope (Carl Zeiss, Oberkochen, Germany). The software used to obtain and analyse the images was Zeiss LSM5 (Carl Zeiss). A 40× water-immersion objective was used for isolated tubules, and a 20× objective was used for samples collected in hollow rectangle glass capillaries. The system consisted of an inverted microscope, a mixed argon/krypton-ion laser with 458, 477, 488 and 514 nm lines and helium–neon lasers with 543 and 633 nm lines. For measurement of rhodamine 123, the 514 nm laser line, a 458/514 nm dichroic filter and a 530–600 nm band pass emission filter were employed. For measurement of daunorubicin, the 543 nm laser line, a 488/543 nm dichroic filter and a 560 nm long-pass emission filter were employed. For measurement of fluorescein, the 488 nm laser line, a 488 nm dichroic filter and a 505–550 nm band pass emission filter were employed. For measurement of quinacrine, the 458 nm laser line, a 488 nm dichroic filter and a 505 nm long-pass emission filter were employed. The Texas Red (sulphorhodamine 101) absorbance spectrum extends between 500 nm and 650 nm, with a primary peak at ~600 nm and a secondary peak at ~550 nm. Previous studies of Texas Red transport using CLSM have used either the 529 nm Ar ion laser line (Miller et al., 1998) or the 568 nm krypton ion laser line (Miller et al., 2001). These lines were not available on our system, and we used the 543 nm He–Ne laser line with a 488/543 nm dichroic filter and 560 nm long-pass emission filter. Because of the high concentrations of Texas Red in secreted fluid droplets (4–400 μmol l^{-1}; see Results), the 514 nm Ar/Kr laser line with a 458/514 nm dichroic filter could also be used.

CLSM of isolated Malpighian tubules

Tubules in the chamber were viewed under reduced, transmitted light illumination, and a field containing 20–30 cells was selected. The focus was adjusted so that the optical slice was through the centre of the lumen. Then, in confocal fluorescence mode, two successive 8-s scans of the field were collected. Laser power was adjusted to minimize photobleaching, as determined from a decline in fluorescence intensity of the second image relative to the first. The confocal image (512×512 pixels) was viewed on a high-resolution monitor, and fluorescence intensity was determined as the mean value for five regions of interest of 200–500 pixels selected in the cellular and luminal compartments and adjacent bathing saline. Detector gain and offset were adjusted so that fluorescence intensity was ~2000 in the lumen on a scale of 0–4095 (12 bits) and the pinhole was set to ~75 μm, corresponding to an optical slice thickness of ~10 μm. Laser power was reduced to minimize photobleaching, and detector gain was adjusted so that when the average pixel intensity in the tubule lumen was ~2000, MT autofluorescence was undetectable.

Data analysis

Data are expressed as means ± S.E.M., unless otherwise indicated. Student's *t*-test was used to evaluate statistical significance, and means were considered significantly different when $P<0.05$. Kinetic parameters describing maximal dye flux (J_{max}), maximal secreted fluid dye concentration ($[Dye]_{sf,max}$), and the bathing saline dye concentrations corresponding to half maximal flux or secreted fluid dye concentration (K_t) were calculated from concentration–response curves fitted by non-linear regression to the Michaelis–Menten equation (SigmaPlot 2000, SPSS Inc., Chicago, IL, USA).

Results

CLSM of isolated Malpighian tubules

Representative confocal microscopic images of cricket and *Drosophila* MTs bathed in saline containing Texas Red are shown in Fig. 1. Approximately 5–10% of the tubules dissected from crickets were similar to those shown in Fig. 1A. The fluorescence intensity (*FI*) profile showed that concentrations of Texas Red in the cells and lumen were elevated above the bath concentration (Fig. 1B). Both cellular and luminal compartments were clearly visible in Fig. 1A, and *FI* could be measured readily in selected regions of interest. In most tubules, however, either the lumen (Fig. 1C) or both the cells and the lumen (Fig. 1D) were not clearly visible because of the presence of numerous opaque concretions. The presence of concretions and extensive apical microvilli also complicated the selection of suitable regions of interest in the lumen. As seen in Fig. 1C,D, *FI* at the periphery of the lumen was often distinctly greater (i.e. brighter) than that in more central regions. Images of *Drosophila* MTs isolated from either adults (Fig. 1E) or larvae (Fig. 1F) were also generally unsuitable for measurements of *FI* because of the presence of cellular and/or luminal concretions.

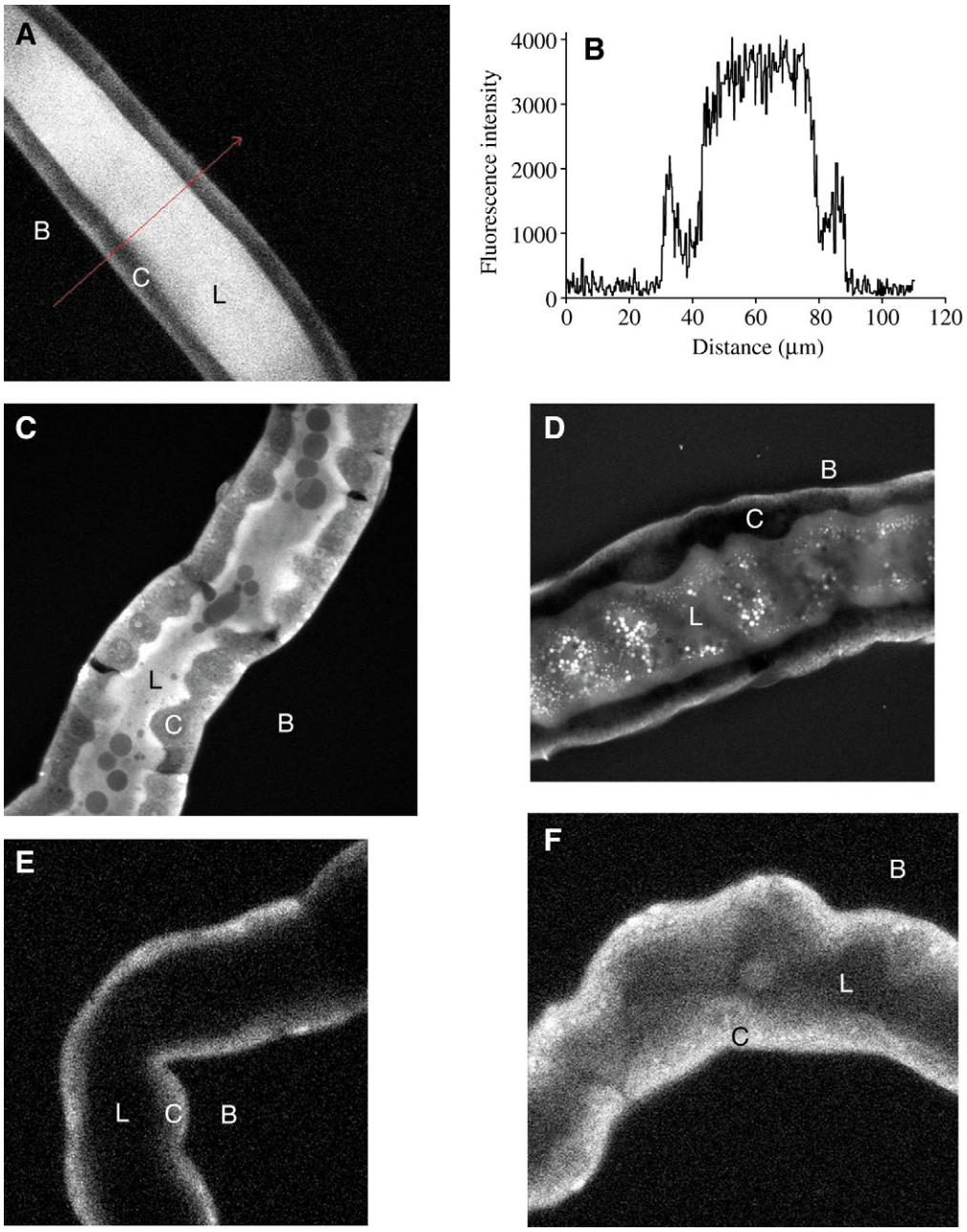

Fig. 1. CLSM images showing accumulation of Texas Red in the lumen and/or cells of Malpighian tubules isolated from crickets (A–D), adult *Drosophila* (E) or larval *Drosophila* (F). The bathing saline (B), lumen (L) and cells (C) are indicated in each image. Tubules were bathed in 10 μmol l^{-1} Texas Red for 15–30 min before each image was recorded. Tubule diameter is ~60 μm in A–C and 35 μm in D,E. Panel B shows the fluorescence intensity profile from the base to the tip of the 110 μm-long arrow in A. Note the presence of large (C) or small (D) spherical concretions in the lumen of the cricket tubules. Some of the concretions in D appear to accumulate high concentrations of Texas Red and appear white whereas others are dark or opaque. The presence of large numbers of small intracellular concretions prevents clear distinction of luminal from cellular compartments in *Drosophila* tubules (E,F).

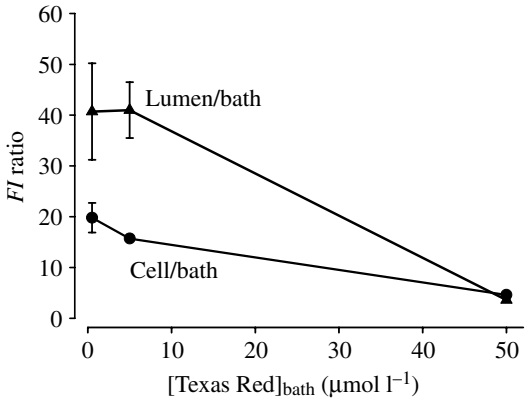

For cricket tubules similar to those shown in Fig. 1A, *FI* was measured in the bath, cells and lumen. Plots of *FI* ratio indicated that Texas Red was approximately 40-fold more concentrated in the lumen relative to the bath when the concentration of Texas Red in the bath was 0.5 or 5 μmol l^{-1} (Fig. 2). The concentration of Texas Red in the cells was

Fig. 2. Fluorescence intensity (*FI*) ratios for cells *versus* bath (circles) and lumen *versus* bath (triangles) as functions of the concentration of Texas Red in the saline bathing isolated cricket Malpighian tubules. An *FI* ratio for each site was calculated from the mean of five *FI* measurements in the bathing saline, cells and lumen. Each data point is the mean (± S.E.M.) ratio for 5–6 widely separated regions in three tubules.

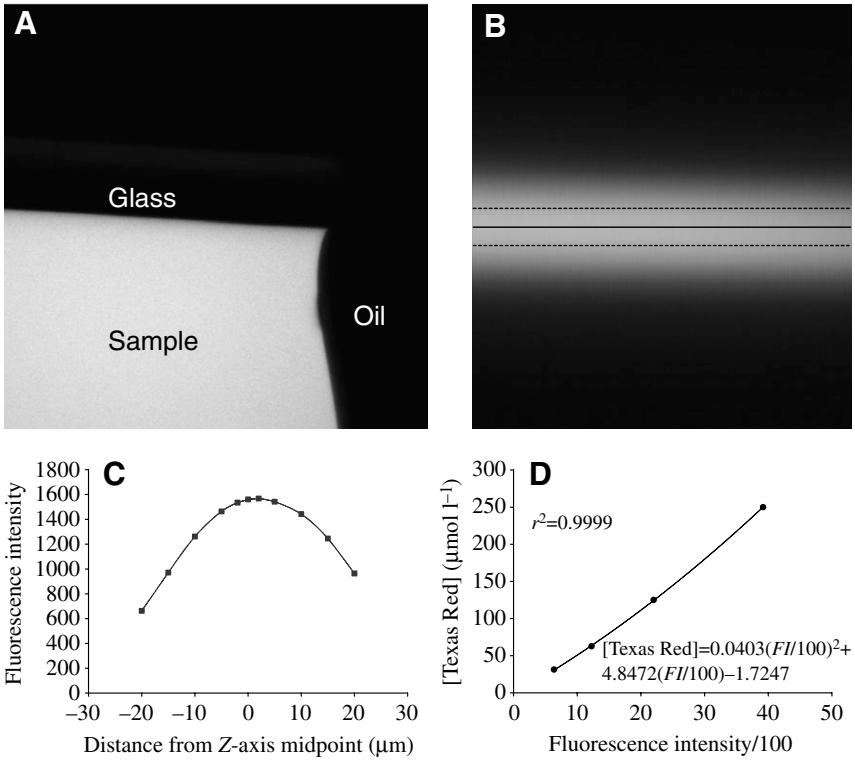

Fig. 3. Analysis of fluorescent fluid samples collected in optically flat hollow rectangle glass capillaries. (A) *X–Y* image of a sample of 50 μmol l^{-1} Texas Red collected under paraffin oil in a hollow rectangle glass capillary. The width of the image is ~250 μm. (B) *X–Z* image of a sample of 125 μmol l^{-1} Texas Red. The solid line was positioned at the apparent midline of the bright band of fluorescence, corresponding to the *Z*-axis midpoint. For comparison, the upper and lower dotted lines indicate positions 10 μm from the apparent *Z*-axis midpoint. The dotted lines are clearly well away from the midline of the bright band in the *X–Z* image and are shown to indicate that the *Z*-axis midpoint can be reliably judged by eye. (C) Fluorescence intensity of *X–Y* images collected for the same sample at the *Z*-positions indicated. The curve shows that fluorescent intensity is nearly constant when the optical slice is positioned within ~5 μm of the apparent *Z*-axis midpoint. (D) Representative calibration curve relating fluorescence intensity to the concentration of Texas Red in fluid samples collected in optically flat glass capillaries. Texas Red concentrations are plotted on the *Y*-axis so that the equation of the curve fit to the data by non-linear regression analysis allows calculation of the dye concentration of experimental samples from the measured fluorescence intensities. Measured fluorescence intensities were divided by 100 for convenience of the curve-fitting calculations. For the curve shown, CLSM detector gain was adjusted so that a near maximal signal (~3900 on a scale of 0–4095) was obtained from the highest concentration (250 μmol l^{-1}) of Texas Red in this series of four calibration samples.

approximately 15–20-fold more concentrated than the bath over the same range of bathing saline Texas Red concentrations. Both lumen/bath and cell/bath *FI* ratios declined to ~4 at bathing saline concentrations of 50 μmol l^{-1}, which is consistent with the presence of saturable mechanisms of Texas Red transport in the MTs.

The widespread occurrence of cellular and luminal concretions in the MTs of crickets, and variations in *FI* between central and peripheral regions of the lumen, complicated the use of isolated tubules for quantitative analysis of Texas Red transport. Analysis of isolated tubules of crickets and *Drosophila* in the presence of the P-gp substrates rhodamine 123 and daunorubicin showed no clear evidence of dye accumulation in the lumen, although the dyes were taken up into the cells (data not shown).

CLSM of fluid samples collected in hollow rectangle glass capillaries

Because of concerns that the concretions in the cells or lumen of the tubules of *Drosophila* and many other species (e.g. Wessing and Zierold, 1999) would confound both quantitative and qualitative analysis of dye accumulation in the tubule lumen, we developed a method for measuring the concentration of Texas Red, daunorubicin and other fluorochromes in the fluid secreted by MTs set up in Ramsay assays. Secreted fluid droplets were collected in optically flat glass capillaries, as described in the methods. Fig. 3A shows a sample of fluid containing Texas Red. The plane of focus was adjusted so that the optical slice comprised approximately the middle 50% of the light path along the *Z*-axis. For capillaries with a path length of 50 μm, a slice thickness of 28 μm was used. For capillaries with a 20 μm path length, pinhole diameter was reduced for a slice thickness of 10 μm. The sensitivity of *FI* measurement was maximized by using thick optical slices for CLSM analysis of secreted fluid samples collected in hollow rectangle capillaries. The choice of slice thickness represented a compromise between two factors. Reducing the thickness of optical slices by decreasing pinhole diameter facilitated positioning of the optical slice at the *Z*-axis midpoint of the light path through the glass capillary, but *FI* also declined linearly as the optical slice thickness was reduced.

Two methods were used to position the optical slice at the *Z*-axis midpoint of the fluid in the capillary. In the first method, a series of *X–Y* images was collected at intervals along the *X*-axis using the *Z*-stack feature of the LSM 510 software. The first and last slices of the stack were selected by manually focusing just outside the upper and lower surfaces of the capillary. A pinhole corresponding to a slice thickness of 28 μm was selected, and a *Z*-stack of 10 images at 5 μm intervals was then collected. A region of interest (ROI) corresponding to 50–100% of the fluorescent region within the image was then selected, and the *FI* of each slice of the *Z*-stack was determined. Fluorescence intensity was maximal for 2–3

slices near the middle of the stack, and the maximal values were used to calculate the fluorochrome concentration from the corresponding calibration curve (described below). The first method typically required 60–100 s to scan a complete stack.

To facilitate more rapid analysis of 25–50 capillaries typically used in each experiment, a second method was developed. The microscope was initially focused approximately in the middle of the fluid within the capillary. An *X–Z* scan was then done, based on 20 slices at 4 μm or 5 μm intervals. The images were thus collected from some distance below, through and above the column of fluid in the capillary. Using the LSM software, the plane of focus was then adjusted to the *Z*-axis midpoint of the column of fluid by moving the horizontal line corresponding to the plane of focus until the band of fluorescence in the *X–Z* image was divided into two mirror images. Fig. 3B shows the images of *X–Z* scans made at the apparent midline of the image, defined as a *Z*-position of 0 μm. Fig. 3B also shows the *X–Z* scans made when the plane of focus was adjusted 10 μm above or below the midline. A series of *X–Y* images were then collected over a range of *Z*-positions, and a plot of *FI* as a function of *Z*-position is shown in Fig. 3C. The plot shows that *FI* in the *X–Y* images varied by less than 5% when the plane of focus was set 5 μm above or below the apparent midline. With practice, the plane of focus could be adjusted to within 1–2 μm of the position corresponding to the maximum *FI*. Fluorescence intensity declined at distances greater than 10 μm from the *Z*-axis middle of the column of fluid within the capillary (Fig. 3C), consistent with inclusion of part of the upper or lower glass wall of the capillary in the optical section.

After the optical slice was adjusted to the *Z*-axis midpoint of the fluid column within the glass capillary, a time series of two *X–Y* images was collected. Using the 20× objective, the samples typically filled 25–75% of the *X–Y* image, corresponding to ~60 000–200 000 pixels. The mean *FI* for the sample was subsequently calculated using the ROI feature of the LSM software. Laser strength was adjusted to avoid any photobleaching, evident as a decline in mean *FI* of the second image relative to the first.

Concentrations of dyes in secreted fluid samples collected in hollow rectangle glass capillaries were calculated from a calibration curve constructed for each experiment. The curve was based on *FI* measurements of samples of known dye concentrations that bracketed the range of interest. For most experiments, four calibration droplets whose concentrations extended over an 8-fold range were used. Detector gain and offset were adjusted so that the *FI* (0–4095, 12 bit) in the highest concentration was ~3900. For concentration–response curves, several sets of calibration samples were required to bracket the wide range of dye concentrations in the secreted droplets. Fig. 3D shows a representative calibration curve for Texas Red. Each curve relating *FI* to dye concentration was fitted by regression analysis. Although the relationship of *FI* to dye intensity was approximately linear (r^2>0.8), fits with r^2 values near unity (r^2>0.999) were obtained for 2nd or 3rd order polynomials. The non-linearity was attributable to self-quenching of the dye at higher concentrations. Preliminary experiments revealed that fluid secretion rates and secreted fluid dye concentrations could vary as much as twofold on different days due to variations in room temperature (17–23°C). Concentration–response curves in the Results below were therefore done in the same assay dish with equal numbers of tubules at each concentration on each day to avoid any bias as a result of differences in temperature.

Ramsay assays: secretion of Texas Red

Concentration–response curves for secreted fluid Texas Red concentration as a function of bathing saline Texas Red concentration for cricket tubules are shown in Fig. 4. The inset in Fig. 4 shows the ratio of Texas Red concentration in the secreted fluid to that in the bathing medium (S/M) as a function of bathing saline Texas Red concentration. The value of S/M for bath Texas Red concentrations of 0.1–1 μmol l^{-1} was in the range of 30–40, similar to the value of ~40 for the lumen/bath *FI* ratio in isolated MTs (Fig. 2). Secreted fluid Texas Red concentration declined at a bath concentration of 50 μmol l^{-1}, and experiments with *Drosophila* tubules described below suggest that high concentrations of the dye are toxic. The data point at 50 μmol l^{-1} was therefore excluded from the curve-fitting procedure used to estimate the kinetic parameters. The length of cricket tubules varies within and between animals, so fluid secretion rates were not calculated in most experiments. However, an approximate flux can be calculated from an estimate of fluid secretion rates of 53 tubules from three insects

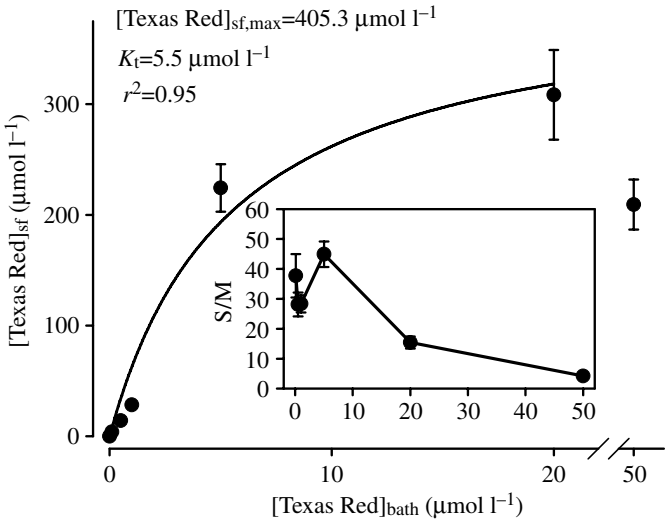

Fig. 4. Secreted fluid Texas Red concentration ([Texas Red]$_{sf}$) as a function of bathing saline Texas Red concentration for cricket tubules set up in Ramsay assays. Each point shows the mean ± S.E.M. for *N*=6–13 tubules. The solid line represents the fit to the Michaelis–Menten equation by non-linear regression analysis. As discussed in the text, the point at 50 μmol l^{-1} Texas Red was excluded from the curve-fitting procedure. The inset shows the ratio of the concentration of Texas Red in the secreted fluid to that in the bathing medium (S/M) as a function of bathing medium Texas Red concentration.

(0.40±0.04 nl min^{-1}). Using the latter value, a maximum flux of 163 fmol min^{-1} tubule^{-1} is estimated at the maximum secreted fluid concentration of 405 μmol l^{-1}.

Concentration–response curves for Texas Red flux across *Drosophila* MTs and corresponding S/M ratios are shown as functions of bathing saline Texas Red concentration in Fig. 5. Both fluid secretion rate and secreted fluid dye concentration declined in saline containing 50 μmol l^{-1} Texas Red relative to the values at lower concentrations, so the data point at 50 μmol l^{-1} Texas Red was excluded from the curve-fitting analysis used to estimate the kinetic parameters J_{max} and K_t. The S/M ratios for *Drosophila* tubules were somewhat lower than those observed for crickets, in the range of 20–30 for bathing saline Texas Red concentrations between 0.1 μmol l^{-1} and 5 μmol l^{-1}.

Secretion of fluorescent P-gp substrates

S/M ratios and concentration–response curves for secreted fluid rhodamine 123 concentration in fluid secreted by isolated cricket tubules are shown in Fig. 6. Cricket tubules stopped secreting fluid after 15–30 min in saline containing 10 μmol l^{-1} or 50 μmol l^{-1} rhodamine 123. For *Drosophila* tubules, it was not feasible to calculate J_{max} and K_t for rhodamine 123 flux because fluid secretion rates declined for all bathing saline concentrations of rhodamine 123 above 0.1 μmol l^{-1}. Fluid secretion by *Drosophila* tubules was completely inhibited by 10 μmol l^{-1} rhodamine 123 and was reduced to 0.09±0.02 nl min^{-1} (N=10) in 0.5 μmol l^{-1} rhodamine 123, approximately 20% of the control value. The S/M ratios for *Drosophila* tubules in 0.1 and 0.5 μmol l^{-1} rhodamine 123 were 35.3±3.6 (N=36) and 11.9±2.7 (N=10), respectively.

By contrast, fluid secretion rates for tubules of both species were maintained in the presence of daunorubicin at concentrations as high as 50 μmol l^{-1} for *Drosophila* and 100 μmol l^{-1} for crickets. S/M ratios and concentration–response curves for secreted fluid daunorubicin concentration in fluid secreted by cricket tubules as a function of bathing saline daunorubicin concentration are shown in Fig. 7. S/M ratios and concentration–response curves for daunorubicin flux across *Drosophila* tubules are shown in Fig. 8.

Secretion of the organic anion fluorescein

Fluorescein is a substrate of organic anion transporters in tubules of *Drosophila* and other species (Neufeld et al., 2005; Bresler et al., 1990). We wished to compare transport of smaller, more hydrophilic organic anions such as fluorescein with the transport of larger, amphiphilic MRP2 substrates such as Texas Red. S/M ratios and concentration–response curves for fluorescein flux are shown in Fig. 9. It is worth noting that J_{max} for fluorescein transport is ~2.5-fold higher than that for Texas Red, but the value of K_t is ~4.5-fold higher than that of Texas Red. As a consequence, the transport efficiency (J_{max}/K_t) for Texas Red is 1.8-fold higher than that for fluorescein.

Effects of MRP2 inhibitors on transport of Texas Red

Transport of Texas Red was reduced by the MRP2-specific inhibitor MK-571 (van Aubel et al., 1998) in tubules of both *Drosophila* (Fig. 10A) and crickets. High concentrations of MK-571 (⩾10 μmol l^{-1}) inhibited fluid secretion by *Drosophila* tubules. There was no effect of 2 μmol l^{-1} MK-571 on fluid secretion rates of 0.67±0.12 nl min^{-1} (N=7) and 0.60±0.05 nl min^{-1} (N=9) in control and experimental groups, respectively. Texas Red flux for tubules bathed in 0.1 μmol l^{-1}

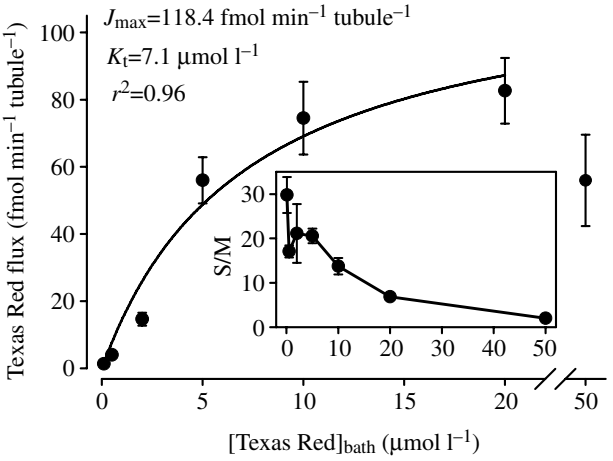

Fig. 5. Transepithelial flux of Texas Red as a function of bathing saline Texas Red concentration for *Drosophila* tubules set up in Ramsay assays. Each point shows the mean ± S.E.M. for N=7–30 tubules. The solid line represents the fit to the Michaelis–Menten equation by non-linear regression analysis. The inset shows the ratio of the concentration of Texas Red in the secreted fluid to that in the bathing medium (S/M) as a function of bathing medium Texas Red concentration. As discussed in the text, the point at 50 μmol l^{-1} Texas Red was excluded from the curve-fitting procedure.

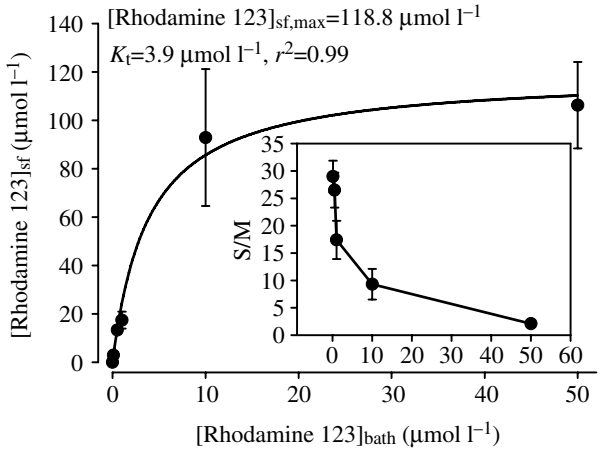

Fig. 6. Secreted fluid rhodamine 123 concentration as a function of bathing saline rhodamine 123 concentration for cricket tubules set up in Ramsay assays. Each point shows the mean ± S.E.M. for N=6–28 tubules. The solid line represents the fit to the Michaelis–Menten equation by non-linear regression analysis. The inset shows the ratio of the concentration of rhodamine 123 in the secreted fluid to that in the bathing medium (S/M) as a function of bathing medium rhodamine 123 concentration.

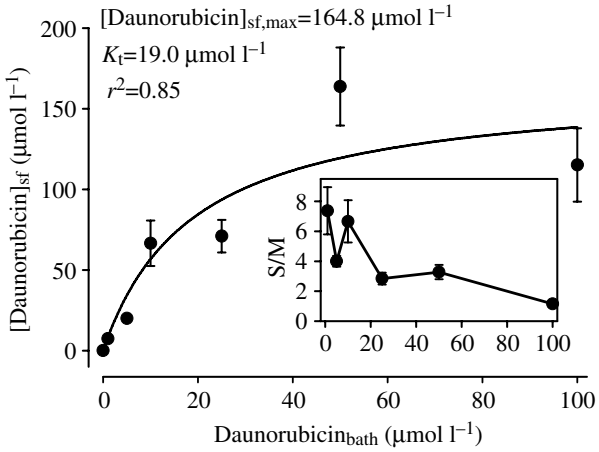

Fig. 7. Secreted fluid daunorubicin concentration as a function of bathing saline daunorubicin concentration for cricket tubules set up in Ramsay assays. Each point shows the mean ± S.E.M. for N=5–8 tubules. The solid line represents the fit to the Michaelis–Menten equation by non-linear regression analysis. The inset shows the ratio of the concentration of daunorubicin in the secreted fluid to that in the bathing medium (S/M) as a function of bathing medium daunorubicin concentration.

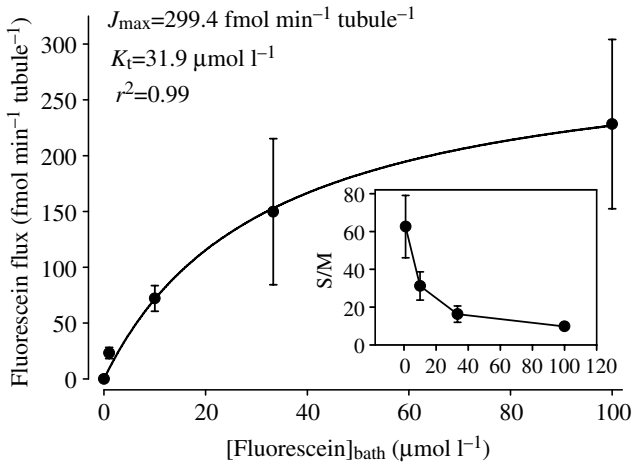

Fig. 9. Transepithelial flux of fluorescein as a function of bathing saline fluorescein concentration for isolated *Drosophila* tubules set up in Ramsay assays. Each point shows the mean ± S.E.M. for N=5 tubules. The solid line represents the fit to the Michaelis–Menten equation by non-linear regression analysis. The inset shows the ratio of the concentration of fluorescein in the secreted fluid to that in the bathing medium (S/M) as a function of bathing medium fluorescein concentration.

Texas Red was reduced 37% by 2 μmol l^{-1} MK-571 (Fig. 10A). For cricket tubules, fluid secretion rates of control (0.48±0.07 nl min^{-1}; N=8) and experimental (0.63±0.10 nl min^{-1}; N=7) groups were unaffected by 10 μmol l^{-1} MK-571. However, secreted fluid Texas Red concentration of cricket tubules bathed in 0.5 μmol l^{-1} Texas Red was reduced by 68%, from 18±2.1 μmol l^{-1} in control saline to 5.7±1.7 μmol l^{-1} in the presence of 10 μmol l^{-1} MK-571.

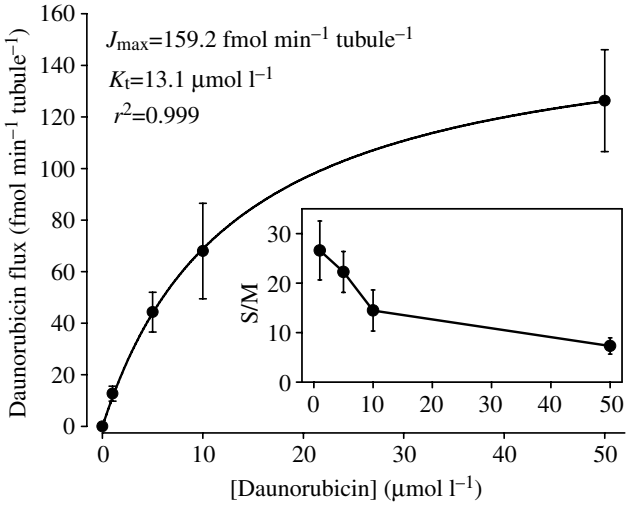

Fig. 8. Transepithelial flux of daunorubicin as a function of bathing saline daunorubicin concentration for *Drosophila* tubules set up in Ramsay assays. Each point shows the mean ± S.E.M. for N=5 tubules. The solid line represents the fit to the Michaelis–Menten equation by non-linear regression analysis. The inset shows the ratio of the concentration of daunorubicin in the secreted fluid to that in the bathing medium (S/M) as a function of bathing medium daunorubicin concentration.

Transport of Texas Red was also inhibited by probenecid (Fig. 10B,C). The concentration of 114.7±5.4 μmol l^{-1} (N=10) Texas Red in fluid secreted by *Drosophila* tubules bathed in saline containing 5 μmol l^{-1} Texas Red was reduced by 63%, to 42.0±7.2 μmol l^{-1}, in the presence of 1000 μmol l^{-1} probenecid (Fig. 10B). However, fluid secretion rate was also reduced significantly, from 0.39±0.06 nl min^{-1} in the controls to 0.26±0.05 nl min^{-1} in the presence of probenecid. The 78% reduction in Texas Red flux was thus partly due to the effects of probenecid on fluid secretion rate, which suggested non-specific effects of the drug at this concentration. At a lower concentration of 200 μmol l^{-1} probenecid, the flux of 0.5 μmol l^{-1} Texas Red was reduced by 43% (Fig. 10C) and there was no significant effect on fluid secretion rate.

Although probenecid is a known inhibitor of both MRP2 and also Na^+-dependent organic anion transport systems (Horikawa et al., 2002), transport of Texas Red was not reduced in Na^+-free saline. In salines containing 5 μmol l^{-1} Texas Red, the concentration of the dye in the secreted fluid was 92±16 μmol l^{-1} (N=10) for tubules in control saline and 105±5 μmol l^{-1} for tubules in Na^+-free saline. Texas Red flux was 62.9±14.5 fmol min^{-1} tubule^{-1} in control saline and 52.3±5.0 fmol min^{-1} tubule^{-1} in Na^+-free saline. The differences are not significant (P>0.05).

Secretion of the organic cation quinacrine

We examined transport of quinacrine by *Drosophila* tubules because it is both a P-gp modulator and it is also a substrate or inhibitor of organic cation transporters such as rOCT2 (Sweet

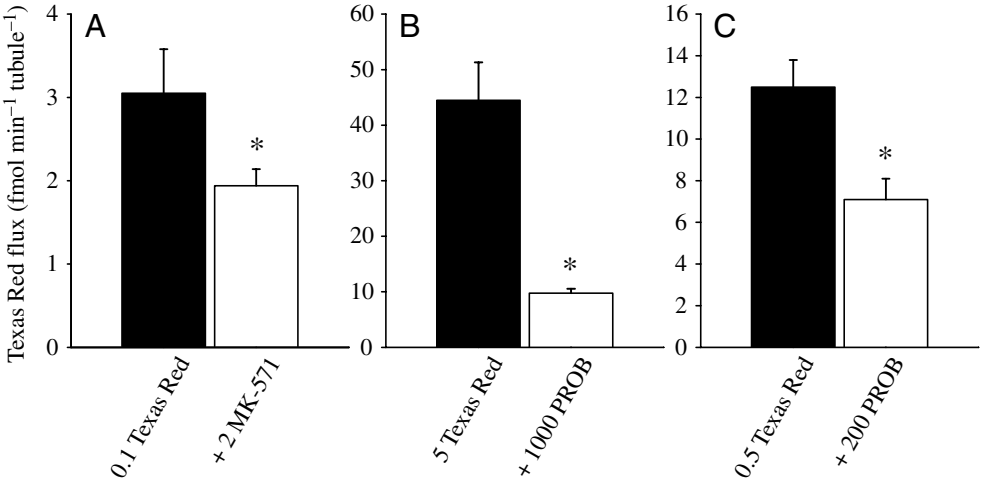

Fig. 10. Effects of the MRP2 inhibitors MK-571 and probenecid (PROB) on transepithelial flux of Texas Red across isolated *Drosophila* tubules set up in Ramsay assays. Each bar shows the flux (mean + S.E.M.) for 7–9 tubules (MK-571) or 10 tubules (probenecid) bathed in saline containing the indicated concentration (μmol l^{-1}) of Texas Red in the absence (filled bars) or presence (open bars) of the indicated inhibitor. Asterisks indicate significant (P<0.05) decreases in flux in the presence of each drug, relative to the corresponding controls.

and Pritchard, 1999; Dohgu et al., 2004). Kinetic analysis showed that the J_{max} for transport was 27.7 fmol min^{-1} tubule^{-1} and the associated K_t was 21.4 μmol l^{-1} (Fig. 11).

Although quinacrine may itself be transported by the organic cation transport system or by P-gps in other cells, neither the P-gp inhibitor verapamil nor the OCT substrate tetraethylammonium (TEA) reduced the flux of quinacrine by *Drosophila* tubules. Transepithelial quinacrine flux across tubules bathed in saline containing 5 μmol l^{-1} quinacrine and 500 μmol l^{-1} verapamil (5.99±0.72 fmol min^{-1} tubule^{-1}; N=10) did not differ from those of the corresponding controls in 5 μmol l^{-1} quinacrine alone (6.31±0.77 fmol min^{-1} tubule^{-1}; N=9). Similarly, transepithelial quinacrine flux across tubules bathed in saline containing 5 μmol l^{-1} quinacrine and 500 μmol l^{-1} TEA (4.28±0.78 fmol min^{-1} tubule^{-1}; N=10) did not differ from those of the corresponding controls (3.72±0.66 fmol min^{-1} tubule^{-1}; N=10). There was no effect of verapamil or TEA on fluid secretion rate or the concentration of quinacrine in the secreted fluid (data not shown).

Effects of p-glycoprotein inhibitors on transport of daunorubicin and rhodamine 123

The concentration of daunorubicin in the fluid secreted by cricket tubules bathed in saline containing the dye (5 μmol l^{-1}) was reduced 71% by 100 μmol l^{-1} verapamil (Fig. 12A) but was unaffected by 100 μmol l^{-1} TEA (Fig. 12B). The concentration of rhodamine 123 in the fluid secreted by cricket tubules bathed in saline containing the dye (0.5 μmol l^{-1}) was reduced 60% by 100 μmol l^{-1} verapamil (Fig. 12C) but was unaffected by 100 μmol l^{-1} TEA (Fig. 12D).

The fluxes of daunorubicin across *Drosophila* tubules bathed in salines containing 1 μmol l^{-1} and 5 μmol l^{-1} daunorubicin were reduced 67% and 64%, respectively, by the P-gp inhibitor verapamil at a concentration of 500 μmol l^{-1} (Fig. 13A,B). Flux of daunorubicin across tubules bathed in saline containing 5 μmol l^{-1} daunorubicin was reduced 44% by verapamil at 100 μmol l^{-1} (Fig. 13C) but was not significantly reduced by the drug at a concentration of 20 μmol l^{-1} (Fig. 13D). For *Drosophila* tubules bathed in 0.5 μmol l^{-1} daunorubicin, the transepithelial flux of the dye was reduced 46% by 50 μmol l^{-1} quinacrine (Fig. 13E). Transepithelial fluxes of 5 μmol l^{-1} daunorubicin were reduced 29% by 1000 μmol l^{-1} of the organic cation TEA (Fig. 13F). Transepithelial flux of rhodamine 123 was unaffected by high concentrations (1000 μmol l^{-1}) of verapamil (Fig. 13G) but was reduced 64% by 1000 μmol l^{-1} TEA (Fig. 13H).

Discussion

Our results show that fluorescent substrates of p-glycoproteins and multidrug-resistance associated protein 2 are secreted by the MTs of two insects, the fruit fly *Drosophila melanogaster* and the cricket *Teleogryllus*

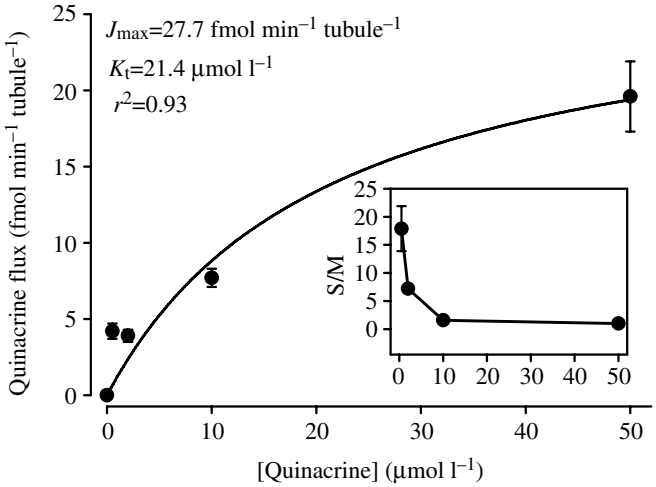

Fig. 11. Transepithelial flux of quinacrine as a function of bathing saline quinacrine concentration for isolated *Drosophila* tubules set up in Ramsay assays. Each point shows the mean ± S.E.M. for N=5 tubules. The solid line represents the fit to the Michaelis–Menten equation by non-linear regression analysis. The inset shows the ratio of the concentration of quinacrine in the secreted fluid to that in the bathing medium (S/M) as a function of bathing medium quinacrine concentration.

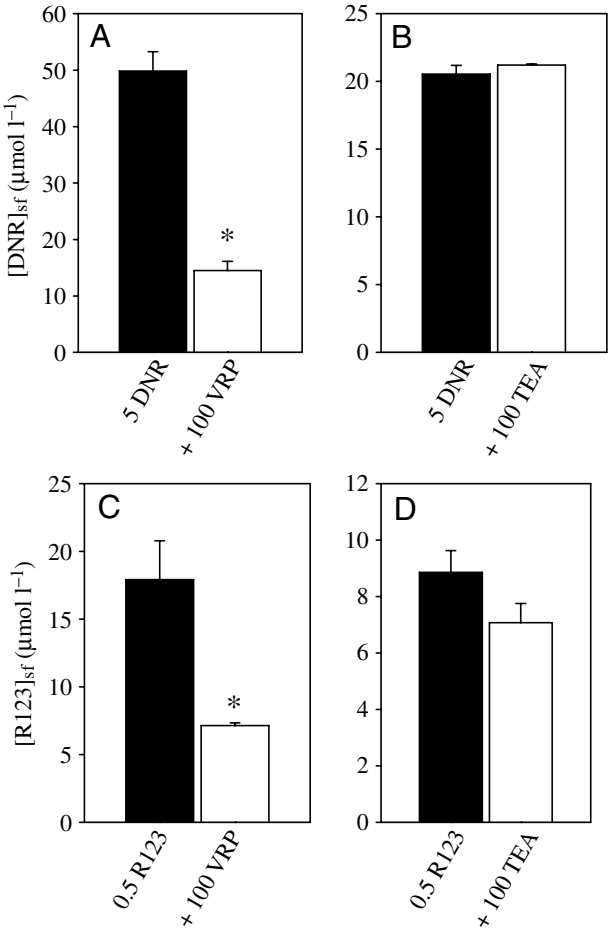

Fig. 12. Effects of p-glycoprotein (P-gp) inhibitors on secreted fluid concentration of daunorubicin (A,B) or rhodamine 123 (C,D) for cricket tubules set up in Ramsay assays. Each panel shows the flux (mean + S.E.M.) for control tubules (filled bars) exposed to the dye alone at the indicated concentration (μmol l^{-1}) and those treated with the same dye concentration and a P-gp inhibitor at the concentration (μmol l^{-1}) indicated (open bars). Abbreviations: daunorubicin (DNR), verapamil (VRP), rhodamine 123 (R123); tetraethylammonium (TEA). Significant differences (P<0.05) between control and experimental groups indicated by asterisks. N=7–10 tubules for each bar.

commodus. The results are significant in two respects. Firstly, we provide the first measurements of transepithelial flux of P-gp and MRP substrates across insect MTs. Flux is calculated as the product of fluid secretion rate and secreted fluid dye concentration. Previous studies of P-gp-like transport by *Manduca* tubules used perfused rather than freely secreting tubules (Gaertner et al., 1998), and studies of MRP2 transporters in crickets and cockroaches measured luminal concentrations of the dye in isolated tubules but did not report corresponding fluid secretion rates (Karnaky et al., 2000, 2001, 2003). Secondly, the collection of secreted fluid samples in optically flat glass capillaries and the measurement of dye concentration in the samples by CLSM may be applicable to other secretory epithelia (salivary and lacrimal glands) or to sub-nanolitre samples of fluid collected by microperfusion or other means.

Transport of MRP2 substrates

Previous studies by Karnaky et al. (2000, 2001, 2003) demonstrated active accumulation of the MRP2 substrates Texas Red and 5-chloromethylfluorescein (CMF) in the cells and lumen of the MTs of crickets (*Acheta domesticus*) and cockroach (*Periplaneta americana*). Texas Red transport is dependent on metabolism and is reduced by the MRP2 inhibitor chlorodinitrobenzene, which does not inhibit transport of chlorophenol red, a substrate for the classic organic anion transporter system. Texas Red transport is unaffected by a 50-fold excess of para-aminohippurate (PAH), a substrate of the organic anion transporter, by TEA, a substrate of the organic cation transporter, or by verapamil, an inhibitor of p-glycoprotein. An apical location of an MRP2-like transporter in cricket MTs has been demonstrated by immunocytochemical staining with an antibody to a sequence of rat MRP2 (Karnaky et al., 2001). However, an apical location of an MRP2-like transporter cannot account for accumulation of Texas Red in the cells of cricket tubules. Cellular accumulation requires an additional mechanism for transport of the dye across the basolateral membrane. The characteristics of such basolateral transport could be assessed in cricket tubules with few or no intracellular concretions (as in Fig. 1A) so that the cytoplasm is relatively translucent and fluorescence intensity could be measured.

Our analyses of both isolated MTs and of secreted fluid samples collected in glass capillaries demonstrated that Texas Red concentrations are elevated 20–40-fold above those in the bathing medium when the latter contains Texas Red at concentrations near or below the K_t values of 5.5 μmol l^{-1} for cricket tubules and 7.1 μmol l^{-1} for *Drosophila* tubules. The typical transepithelial potential across *Drosophila* tubules is 30–45 mV lumen-positive (O'Donnell et al., 1996, 1998), which could only account for a 3–6-fold elevation of the concentration of the anion Texas Red by passive means. The higher S/M ratios measured in the present paper are therefore indicative of active transepithelial transport of Texas Red.

Possibly toxic effects of high concentrations of Texas Red are evident in the reduction of luminal Texas Red concentration in both species and the reduction in fluid secretion rate of *Drosophila* tubules when the concentration of Texas Red in the bathing medium is increased above 20 μmol l^{-1}. By contrast, fluid secretion rate was unaffected by fluorescein at concentrations as high as 100 μmol l^{-1}. In broad terms, the results of our kinetic analyses suggest that Texas Red transport mechanisms are of higher affinity but lower capacity than those responsible for elimination of organic anions such as fluorescein. The finding that high concentrations of Texas Red inhibit fluid secretion provides an important caveat for studies based only on measurement of dye concentrations in the lumen. Measurement of fluid secretion rate not only permits calculation of transepithelial

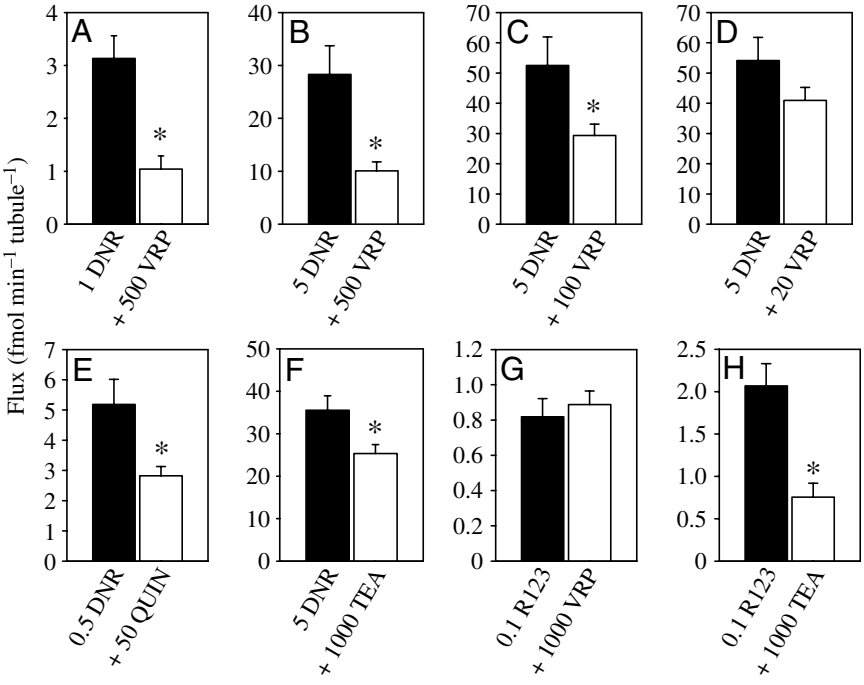

Fig. 13. Effects of p-glycoprotein (P-gp) inhibitors on transepithelial flux of daunorubicin (A–F) or rhodamine 123 (G,H) across *Drosophila* tubules set up in Ramsay assays. Each panel shows the flux (mean + S.E.M.) for control tubules (filled bars) exposed to the dye alone at the indicated concentration (μmol l^{-1}) and those treated with the same dye concentration and a P-gp inhibitor at the concentration (μmol l^{-1}) indicated (open bars). Abbreviations: daunorubicin (DNR), verapamil (VRP), quinacrine (QUIN), rhodamine 123 (R123); tetraethylammonium (TEA). Significant differences (P<0.05) between control and experimental groups indicated by asterisks. N=7–10 tubules for each bar.

dye flux but also provides an independent measurement of the non-specific toxicity of dye substrates or inhibitors (see below).

Transport of Texas Red was inhibited by the MRP2 inhibitors MK-571 and probenecid. Although probenecid inhibits both MRP2 and organic anion transporters, the latter pathway is Na^+ dependent. Secretion of organic anions such as PAH is inhibited 80% by removal of Na^+ from the bathing medium (Linton and O'Donnell, 2000). By contrast, transport of Texas Red was unaffected by Na^+-free conditions. This finding clearly distinguishes transport of Texas Red from that of compounds such as fluorescein and indicates that inhibition by probenecid must therefore reflect an effect upon a transporter distinct from the classic organic anion transport pathway. Reductions of fluid secretion rate by high (1000 μmol l^{-1}) concentrations of probenecid were associated with a 33% reduction in fluid secretion rate. The use of lower concentrations of probenecid permitted inhibition of Texas Red transport to be detected in the absence of any effect on fluid secretion rate. The relative concentrations of substrates and inhibitors that we used are similar to those of previous studies of MRP2. Transport of 0.05 μmol l^{-1} estradiol glucuronide by rabbit MRP2 expressed in Sf9 cells is reduced to 33% of the control value by 5 μmol l^{-1} MK571 (van Aubel et al., 1998). Transport of 3 μmol l^{-1} saquinavir is reduced to 17% of the control value by 75 μmol l^{-1} MK571 (Williams et al., 2002). Transport of 4 μmol l^{-1} *N*-ethylmaleimide glutathione by human MRP2 expressed in *Spodoptera frugiperda* ovarian cells is reduced 50% by 1000 μmol l^{-1} probenecid (Bakos et al., 2000) and transport of 1 μmol l^{-1} methotrexate by a human carcinoma cell line is reduced 50% by 500 μmol l^{-1} probenecid (Hoijberg et al., 1999).

Transport of p-glycoprotein substrates

Previous studies have reported uptake of daunorubicin and rhodamine 123 into the cells but not the lumen of the MTs of the cricket *Acheta domesticus* (Karnaky et al., 2001) and the tobacco hornworm, *Manduca sexta* (Gaertner and Morris, 1999). The latter authors suggested that accumulation of the dyes in the cells is a form of xenobiotic scavenging unrelated to P-gp. Our results, based on collection of secreted fluid, clearly indicate that transepithelial secretions of both rhodamine 123 and daunorubicin are saturable forms of transport that are inhibitable by verapamil and quinacrine. It is possible that species differences underlie the differences between our results and those of Gaertner and Morris (1999) or that the toxic effects of rhodamine 123 noted in both *Drosophila melanogaster* and *Teleogryllus commodus* also apply to the tubules of *Manduca sexta*. Gaertner and Morris (1999) suggested several possible explanations to account for transepithelial transport of 50–5000 μmol l^{-1} nicotine observed in their earlier study (Gaertner et al., 1998), whereas 5–10 μmol l^{-1} daunorubicin and rhodamine 123 were not accumulated in the lumen. In particular, they note the possibility that '*exciting and/or emitted light was quenched, reflected or absorbed by the tissue and opaque uric acid crystals present within the lumen.*' We also noted that it was not feasible to clearly visualize dyes in the lumen of many cricket MTs (*T. commodus*) and all *Drosophila* tubules because of opaque concretions in the cells and/or lumen. A re-examination of the possible secretion of fluorescent P-gp substrates by lepidopteran tubules may be worthwhile, using the method developed here for analysis of secreted fluid samples collected in hollow rectangle glass capillaries. Tubules of the cabbage looper, *Trichoplusia ni*, might be suitable for such study because they secrete fluid at high rates and for

prolonged periods (M. R. Rheault, J. Plaumann and M. J. O'Donnell, unpublished).

Transport of daunorubicin by tubules of both species was reduced by the P-gp inhibitor verapamil, consistent with involvement of a P-gp-like transporter. The relative concentrations of substrate and inhibitor that we have used are broadly similar to those used in previous studies. For example, transport of 1 μmol l^{-1} rhodamine 123 or 3 μmol l^{-1} doxorubicin is reduced ~50% by 20 μmol l^{-1} verapamil in several cell lines (van der Sandt et al., 2000). Transport of 1 μmol l^{-1} daunorubicin is reduced 50% by 10.3 μmol l^{-1} verapamil in lymphocytes (Green et al., 2001). Daunorubicin transport by *Drosophila* tubules is also inhibited by quinacrine, an organic cation that is also a P-gp modulator, and by high concentrations of TEA. A role for both P-gp and organic cation/H^+ exchange has been proposed to account for the effects of daunorubicin transport in flounder renal tubules (Miller, 1995). We suggest that in *Drosophila* tubules as well, daunorubicin may be transported both by P-gp-like transporters and by the organic cation transporters involved in transepithelial secretion of quaternary ammonium compounds such as TEA (Rheault and O'Donnell, 2004).

Analysis of transepithelial transport of rhodamine 123 is complicated by the inhibitory effects of this P-gp substrate on fluid secretion, particularly in the case of isolated *Drosophila* tubules. Transport of rhodamine 123 is saturable in cricket tubules and is inhibited by verapamil. Fluid secretion by *Drosophila* tubules is inhibited by rhodamine 123 at concentrations above 0.1 μmol l^{-1}, and transport at such low concentrations may involve mechanisms distinct from saturable transport by P-gp-like transporters. Moreover, the transport of rhodamine 123 by *Drosophila* tubules is unaffected by very high concentrations of verapamil, again suggesting processes unrelated to P-gp. A further complication is that the principal cells of dipteran tubules retain rhodamine 123 for a short period and the stellate cells reabsorb the dye from the tubule lumen (Meulemans and De Loof, 1992). The dye accumulates in the stellate cell mitochondria and eventually in intensely fluorescing vesicles, probably lysosomes. Endocytotic uptake has been ruled out. In addition, rhodamine 123 precipitates on the luminal concretions in the distal segment of the anterior tubules (Meulemeans and De Loof, 1992). Given the inhibitory effects of rhodamine 123 on fluid secretion rate and the complexities in the routes of transport, we suggest that it is an inappropriate substrate for further analysis of P-gp-like transporters in dipteran MTs.

Transport of the organic cation quinacrine is also saturable, with *Drosophila* tubules accumulating the compound in the lumen at concentrations as high as 17-fold above those in the bath. However, in contrast to quinacrine transport by the rat choroid plexus, transport by *Drosophila* tubules is unaffected by either verapamil or TEA. We had examined the effects of quinacrine on daunorubicin transport because it is a known P-gp modulator (Tiberghien and Loor, 1996). Although we have not examined quinacrine transport in detail, these results suggest that there may be differences in the mechanisms of quinacrine transport in *Drosophila* MTs and vertebrate tissues. Moreover, it appears that the tubules possess a mechanism of organic cation transport distinct from that utilized for the P-gp substrate daunorubicin and the organic cation TEA (Rheault and O'Donnell, 2004).

CLSM analysis of secreted droplets collected in optically flat glass capillaries

Dye concentration in nanolitre samples of secreted fluid droplets collected in optically flat glass capillaries can readily be measured using CLSM. In conjunction with Ramsay assays, these measurements permit calculation of transepithelial dye flux. The Ramsay assays also provide a means for determining the effects of the dyes or transport inhibitors on processes other than dye transport. Rhodamine 123, for example, clearly inhibits fluid secretion by tubules of *Drosophila* and crickets. This finding raises the possibility that in instances where fluid secretion is reduced, any associated reduction in dye transport may reflect impairment of cellular metabolism or other transporters involved in cellular homeostasis. Rhodamine 123 is known as a mitochondrial dye, so its effects on fluid secretion transport may reflect impairment of cell metabolism. Analysis of dye transport solely by image analysis of cellular and luminal compartments would not provide this additional information about the effects of the dye on cell function.

We developed the use of optically flat glass capillaries for analysis of transepithelial dye transport because of concerns that opaque cellular or luminal concretions would block or interfere with laser light transmission. Although we have previously used CLSM for visualization of fluorescein transport by *Drosophila* tubules (Linton and O'Donnell, 2000), the presence of concretions alters the amount of laser light that reaches a given region of the tubule, thereby making quantitative analysis unfeasible. There are also concerns that the concretions move in the lumen during fluid secretion, thereby altering the amount of laser light passing through the lumen, and that cellular concretions may be transferred from cell to lumen under certain conditions (Hazelton et al., 2001). Another advantage of analysis of secreted fluid droplets by CLSM is that laser strength can be optimized to minimize photobleaching but without the additional concerns over the effects of the laser light on cellular components. Low concentrations of fluorochromes can be measured quickly and accurately because fluorescence intensity measurements are based on large numbers of pixels (typically >60 000) relative to isolated tubules and because the thickness of the optical slice can be increased. Estimates of dye concentration are less affected by variations in pH of the cytoplasmic milieu, and the calibration solutions can be adjusted to resemble closely the ionic strength and pH of the secreted fluid. Secreted fluid samples from large numbers of tubules (typically 20 per experiment) in each Ramsay assay can be analysed much more rapidly than is possible if multiple regions of interest within the lumen and bath are selected for analysis in isolated tubules examined by CLSM. It is important to point out that the methods described here for analysis of nanolitre samples of

fluid containing fluorescent transporter substrates provide a faster and cheaper alternative to the use of radiolabelled substrates. Lastly, it is worth noting that, although we have analysed fluid samples collected in hollow rectangle glass capillaries by CLSM, fluorescence intensity could also be measured by epifluorescence microscopy of the capillaries. Transport of fluorescein by isolated tubules of the cricket *A. domesticus* has recently been studied by means of quantitative fluorescence microscopy (Neufeld et al., 2005).

The flux measurements reported here can be used to estimate the time required to clear the haemolymph of a given concentration of dye. Haemolymph volume in *Drosophila* is of the order of 0.1 μl in control flies but is as high as 0.32 μl in desiccation-resistant strains (Folk et al., 2001). For Texas Red, each tubule secretes ~80 fmol min^{-1} when bathed in saline containing the dye at a concentration of 20 μmol l^{-1} (Fig. 5). The four tubules will thus clear the haemolymph content of 2 pmols (=0.1 μl × 20 μmol l^{-1}) of the dye in ~6 min. Similar calculations indicate clearance times of ~10 min for daunorubicin, ~12 min for fluorescein and ~25 min for quinacrine. These estimates suggest that the MTs may play an important role in the elimination of potentially toxic P-gp substrates and MRP2 substrates from the haemolymph.

In summary, our results show that transport of fluorescent substrates analysed by CLSM of secreted fluid samples collected in hollow rectangle glass capillaries indicates the presence of P-gp-like and MRP2-like transporters in the MTs of two insect species. Demonstration of secretion of P-gp and MRP2 substrates by *Drosophila* tubules is of particular interest because of previous molecular genetic evidence for the presence of *MDR* and *MRP* genes in this species (Wu et al., 1991; Tarnay et al., 2004). Our results set the stage for further analysis of the effects of treatments, such as cadmium exposure and heat shock (Tapadia and Lakhotia, 2005), known to alter *MRP* or *MDR* gene expression on transport of P-gp and MRP2 substrates by isolated MTs and the possible role of such transport in insecticide resistance. In view of recent evidence showing modulation of organic cation transport by dietary loading, peptides, amines and intracellular second messengers (Bijelic and O'Donnell, 2005; Bijelic et al., 2005), it will also be of interest to examine whether transport of P-gp and MRP2 substrates is also modulated by such treatments.

References

Ashburner, M. (1989). *Drosophila: A Laboratory Manual.* New York: Cold Spring Harbor Laboratory Press.

Bakos, E., Evers, R., Sinko, E., Varadi, A., Borst, P. and Sarkadi, B. (2000). Interactions of the human multidrug resistance proteins MRP1 and MRP2 with organic anions. *Mol. Pharmacol.* **57**, 760-768.

Bain, L. J. and LeBlanc, G. A. (1996). Interaction of structurally diverse pesticides with the human MDR1 gene product P-glycoprotein. *Toxicol. Appl. Pharmacol.* **141**, 288-298.

Bard, S. M. (2000). Multixenobiotic resistance as a cellular defense mechanism in aquatic organisms. *Aquat. Toxicol.* **48**, 357-389.

Bijelic, G. and O'Donnell, M. J. (2005). Diuretic factors and second messengers stimulate secretion of the organic cation TEA by the Malpighian tubules of *Drosophila melanogaster*. *J. Insect Physiol.* **51**, 267-275.

Bijelic, G., Kim, N. R. and O'Donnell, M. J. (2005). Effects of dietary or injected organic cations on larval *Drosophila melanogaster*: mortality and elimination of tetraethylammonium from the hemolymph. *Arch. Insect Biochem. Physiol.* **60**, 93-103.

Bresler, V. M., Belyaeva, E. A. and Mozhayeva, M. G. (1990). A comparative study on the system of active transport of organic acids in Malpighian tubules of insects. *J. Insect Physiol.* **36**, 259-270.

Buss, D. S., McCaffery, A. R. and Callaghan, A. (2002). Evidence for p-glycoprotein modification of insecticide toxicity in mosquitoes of the *Culex pipiens* complex. *Med. Vet. Entomol.* **16**, 218-222.

Dohgu, S., Yamauchi, A., Takata, F., Sawada, Y., Higuchi, S., Naito, M., Tsuruo, T., Shirabe, S., Niwa, M., Katamine, S. et al. (2004). Uptake and efflux of quinacrine, a candidate for the treatment of prion diseases, at the blood-brain barrier. *Cell Mol. Neurobiol.* **24**, 205-217.

Dow, J. A. T., Maddrell, S. H. P., Görtz, A., Skaer, N. J. V., Brogan, S. and Kaiser, K. (1994). The Malpighian tubules of *Drosophila melanogaster*, a novel phenotype for studies of fluid secretion and its control. *J. Exp. Biol.* **197**, 421-428.

Folk, D. G., Han, C. and Bradley, T. J. (2001). Water acquisition and partitioning in *Drosophila melanogaster*: effects of selection for desiccation-resistance. *J. Exp. Biol.* **204**, 3323-3331.

Gaertner, L. S. and Morris, C. E. (1999). Accumulation of daunomycin and fluorescent dyes by drug-transporting Malpighian tubule cells of the tobacco hornworm, *Manduca sexta. Tissue Cell* **31**, 185-194.

Gaertner, L. S., Murray, C. L. and Morris, C. E. (1998). Transepithelial transport of nicotine and vinblastine in isolated Malpighian tubules of the tobacco hornworm (*Manduca sexta*) suggests a P-glycoprotein-like mechanism. *J. Exp. Biol.* **201**, 2637-2645.

Gerrard, B., Stewart, C. and Dean, M. (1993). Analysis of Mdr50: a *Drosophila* P-glycoprotein/multidrug resistance gene homolog. *Genomics* **17**, 83-88.

Green, L. J., Marder, P. and Slapak, C. A. (2001). Modulation by LY335979 of P-glycoprotein function in multidrug-resistant cell lines and human natural killer cells. *Biochem. Pharmacol.* **61**, 1393-1399.

Hazelton, S. R., Felgenhauer, B. E. and Spring, J. H. (2001). Ultrastructural changes in the Malpighian tubules of the house cricket, *Acheta domesticus*, at the onset of diuresis: A time study. *J. Morphol.* **247**, 80-92.

Hooijberg, J. H., Broxterman, H. J., Kool, M., Assaraf, Y. G., Peters, G. J., Noordhuis, P., Scheper, R. J., Borst, P., Pinedo, H. M. and Jansen, G. (1999). Antifolate resistance mediated by the multidrug resistance proteins MRP1 and MRP2. *Cancer Res.* **59**, 2532-2435.

Horikawa, M., Kato, Y., Tyson, C. A. and Sugiyama, Y. (2002). The potential for an interaction between MRP2 (ABCC2) and various therapeutic agents: probenecid as a candidate inhibitor of the biliary excretion of irinotecan metabolites. *Drug Metab. Pharmacokinet*. **17**, 23-33.

Karnaky, K. J., Jr., Petzel, D., Sedmerova, M., Gross, A. and Miller, D. S. (2000). Mrp2-like transport of Texas Red by Malpighian tubules of the common American cockroach, *Periplaneta americana. Bull. Mt. Des. Isl. Biol. Lab.* **39**, 52-53.

Karnaky, K. J., Jr, Sedmerova, M., Petzel, D., Bridges, J., Boatwright, S. W. and Miller, D. S. (2001). Mrp2-like transport in the Malpighian tubule of the cricket, *Acheta domesticus*. *Bull. Mt. Des. Isl. Biol. Lab.* **40**, 53-55.

Karnaky, K. J., Jr, Hazen-Martin, D. and Miller, D. S. (2003). The xenobiotic transporter, MRP2, in epithelia from insects, sharks, and the human breast: implications for health and disease. *J. Exp. Zool.* **300**, 91-97.

Lanning, C. L., Fine, R. L., Sachs, C. W., Rao, U. S., Corcoran, J. J. and Abou-Donia, M. B. (1996). Chlorpyrifos oxon interacts with the mammalian multidrug resistance protein, P-glycoprotein. *J. Toxicol. Environ. Health* **47**, 395-407.

Linton, S. M. and O'Donnell, M. J. (2000). Novel aspects of the transport of organic anions by the Malpighian tubules of *Drosophila melanogaster*. *J. Exp. Biol.* **203**, 3575-3584.

Meulemans, W. and De Loof, A. (1992). Transport of the cationic fluorochrome rhodamine 123 in an insect's Malpighian tubule: indications of a reabsorptive function of the secondary cell type. *J. Cell Sci.* **101**, 349-361.

Miller, D. S. (1995). Daunomycin secretion by killfish renal proximal tubules. *Am. J. Physiol.* **269**, R370-R379.

Miller, D. S., Masereeuw, R., Henson, J. and Karnaky, K. J., Jr (1998). Excretory transport of xenobiotics by dogfish shark rectal gland tubules. *Am. J. Physiol.* **275**, R697-R705.

Miller, D. S., Graeff, C., Droulle, L., Fricker, S. and Fricker, G. (2001). Xenobiotic efflux pumps in isolated fish brain capillaries *Am. J. Physiol.* **282**, R191-R198.

Murray, C. L., Quaglia, M., Arnason, J. T. and Morris, C. E. (1994). A putative nicotine pump at the metabolic blood-brain barrier of the tobacco hornworm. *J. Neurobiol.* **25**, 23-34.

Neufeld, D. S., Kauffman, R. and Kurtz, Z. (2005). Specificity of the fluorescein transport process in Malpighian tubules of the cricket *Acheta domesticus*. *J. Exp. Biol.* **208**, 2227-2236.

O'Donnell, M. J., Dow J. A. T., Huesmann, G. R., Tublitz, N. J. and Maddrell, S. H. P. (1996). Separate control of anion and cation transport in Malpighian tubules of *Drosophila melanogaster*. *J. Exp. Biol.* **199**, 1163-1175.

O'Donnell, M. J., Rheault, M. R., Davies, S. A., Rosay, P., Harvey, B. J., Maddrell, S. H. P., Kaiser, K. and Dow, J. A. T. (1998). Hormonally-controlled chloride movement across *Drosophila* tubules is via ion channels in stellate cells. *Am. J. Physiol.* **43**, R1039-R1049.

Podsiadlowski, L., Matha, V. and Vilcinskas, A. (1998). Detection of a P-glycoprotein related pump in *Chironomus* larvae and its inhibition by verapamil and cyclosporin A. *Comp. Biochem. Physiol.* **121B**, 443-450.

Rheault, M. R. and O'Donnell, M. J. (2004). Organic cation transport by Malpighian tubules of *Drosophila melanogaster*: application of two novel electrophysiological methods. *J. Exp. Biol.* **207**, 2173-2184.

Sweet, D. H. and Pritchard, J. B. (1999). rOCT2 is a basolateral potential-driven carrier, not an organic cation/proton exchanger. *Am. J. Physiol.* **277**, F890-F898.

Tapadia, M. G. and Lakhotia, S. C. (2005). Expression of mdr49 and mdr65 multidrug resistance genes in larval tissues of *Drosophila melanogaster* under normal and stress conditions. *Cell Stress Chaperones* **10**, 7-11.

Tarnay, J. N., Szeri, F., Ilias, A., Annilo, T., Sung, C., Le Saux, O., Varadi, A., Dean, M., Boyd, C. D. and Robinow, S. (2004). The dMRP/CG6214 gene of *Drosophila* is evolutionarily and functionally related to the human multidrug resistance-associated protein family. *Insect Mol. Biol.* **13**, 539-548.

Tiberghien, F. and Loor, F. (1996). Ranking of P-glycoprotein substrates and inhibitors by a calcein-AM fluorometry screening assay. *Anticancer Drugs* **7**, 568-578.

van Aubel, R. A., van Kuijck, M. A., Koenderink, J. B., Deen, P. M., van Os, C. H. and Russel, F. G. (1998). Adenosine triphosphate-dependent transport of anionic conjugates by the rabbit multidrug resistance-associated protein Mrp2 expressed in insect cells. *Mol. Pharmacol.* **53**, 1062-1067.

van der Sandt, I. C., Blom-Roosemalen, M. C., de Boer, A. G. and Breimer, D. D. (2000). Specificity of doxorubicin versus rhodamine-123 in assessing P-glycoprotein functionality in the LLC-PK1, LLC-PK1:MDR1 and Caco-2 cell lines. *Eur. J. Pharm. Sci*. **11**, 207-214.

Wessing, A. and Zierold, K. (1999). The formation of type-I concretions in *Drosophila* Malpighian tubules studied by electron microscopy and X-ray microanalysis. *J. Insect Physiol.* **45**, 39-44.

Williams, G. C., Liu, A., Knipp, G. and Sinko, P. J. (2002). Direct evidence that saquinavir is transported by multidrug resistance-associated protein (MRP1) and canalicular multispecific organic anion transporter (MRP2). *Antimicrob. Agents Chemother.* **46**, 3456-3462.

Wu, C. T., Budding, M., Griffin, M. S. and Croop, J. M. (1991). Isolation and characterization of Drosophila multidrug resistance gene homologs. *Mol. Cell. Biol.* **11**, 3940-3948.